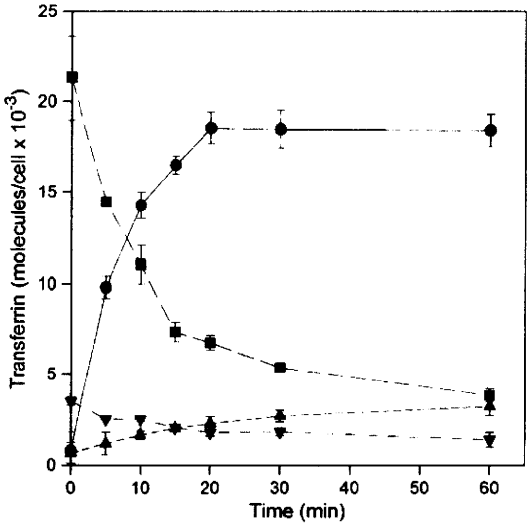

Fig. 3. Time course of Tf efflux. TRVb-TfR2α cells and TRVb mock cells were incubated with 3.5×10^{-7} M [^{125}I]Tf at 37 °C for 1 h, washed to remove unbound Tf, and then acid-washed to remove Tf bound to cell surface receptors. Cells were then incubated at 37 °C for the indicated times, the medium was collected, and solubilized cells were taken for counting. Tf exocytosed into the medium from TRVb-TfR2α cells (●) and TRVb mock cells (▲), and Tf retained in TRVb-TfR2α cells (■) and TRVb mock cells (▼), are shown. Experiments were performed in triplicate.

Tf internalization by TRVb mock cells, in keeping with Tf internalization by TfR2α, as discussed above. Internalized Tf mediated by TfR2α was exocytosed from TRVb-TfR2α cells; approximately 80% of Tf taken up via TfR2α was released by 30 min. The indication is that an effective efflux route exists for Tf taken up by TfR2α, suggesting that TfR2α, like TfR1, is recycled by the cells.

In a further investigation of the TfR2α pathway, the degradation of Tf internalized by TfR2α was determined. After 60 min, approximately 90% of Tf exocytosed from TRVb-TfR2α cells was precipitable by trichloroacetic acid (TCA)/phosphotungstic acid (PTA), indicating that Tf bound to TfR2α has recycled without substantial degradation in cells.

Pulse-chase study

To determine the fraction of cell-membrane-bound Tf that is internalized and the recycling time, we performed a pulse-chase experiment (Supplementary Fig. 2). Almost all Tf initially bound to TfR2α at 4 °C was released into the culture medium after 10 min of incubation at 37 °C, and there was no significant internalization of cell-surface-bound Tf in the single cycle of this pulse-chase study.

Absence of TfR1 TfR2 heterodimers

The effectiveness of anti-FLAG M2 antibody and anti-TfR1 antibody in immunoprecipitation had been confirmed before these experiments were undertaken (data not shown). HuH-7 cells, which express detectable TfR1 by Western blot analysis, were transiently transfected with the TfR2α expression vector, and cell lysates were taken for immunoprecipitation and Western blot analysis (Supplementary Fig. 3). Western blot analysis by anti-TfR1 antibody for the samples without immunoprecipitation showed that HuH-7 cells and HuH-7 cells transfected with TfR2α express almost identical amounts of TfR1. Furthermore, Western blot analysis by anti-TfR2 antibody for the samples not subjected to immunoprecipitation showed that HuH-7 cells transfected with TfR2α express more TfR2α proteins than nontransfected HuH-7 cells. These data indicated that the transiently transfected cells overexpressed TfR2α protein and that the antibodies were highly effective for Western blot analysis. When immunoprecipitation was performed with anti-TfR1 antibody, a band was clearly detected in transfected and nontransfected cells, but no band was found with the anti-TfR2 antibody. If a TfR1 TfR2 heterodimer were present, anti-TfR1 antibody would precipitate that protein, and Western blot analysis with anti-TfR2 antibody would show the band. When immunoprecipitation was performed with anti-FLAG M2 antibody, a 100-kDa band was detected only in transfected cells when the anti-TfR2 antibody was used as the primary antibody in Western blot analysis, indicating that transient transfection resulted in expression of immunoprecipitable TfR2α protein. No band was detected when anti-TfR1 was used as the primary antibody. Prolonged exposure of the blotted membrane to the developing solution did not make a difference. The possibility that the N-terminal FLAG tag in TfR2α interferes with dimer formation is unlikely, since the recombinant TfR1 lacking the first 120 N-terminal intracellular residues spontaneously dimerizes.[17] These results indicate that no detectable heterodimer of TfR1 and TfR2α was formed by the TfR2α-transfected HuH-7 cells. Therefore, our experiments detect TfR2, not the heterodimer of TfR1 and TfR2.

Specificity of detection by AFM

HLF cells (human hepatoma) were transiently cotransfected with TfR2α and green fluorescent protein (GFP) for identification, and tested with a Tf-coated tip. Retraction force curves were recorded with a Tf-coated tip and showed specific unbinding events between Tf on the tip and TfR2α at the cell surface (in Tris-buffered saline, pH 7.4) (Fig. 4a). The probability of binding between the Tf-coated tip and the TfR2 at the cell surface reached 26% ($n=7$ cells). In contrast, when nontransfected cells were tested with a Tf-coated tip, this probability was only 6% ($n=12$ cells, $p<0.001$, t test). This indicated that transient transfection of the TfR2α expression vector was adequate for the investigation using AFM (Fig. 4b).

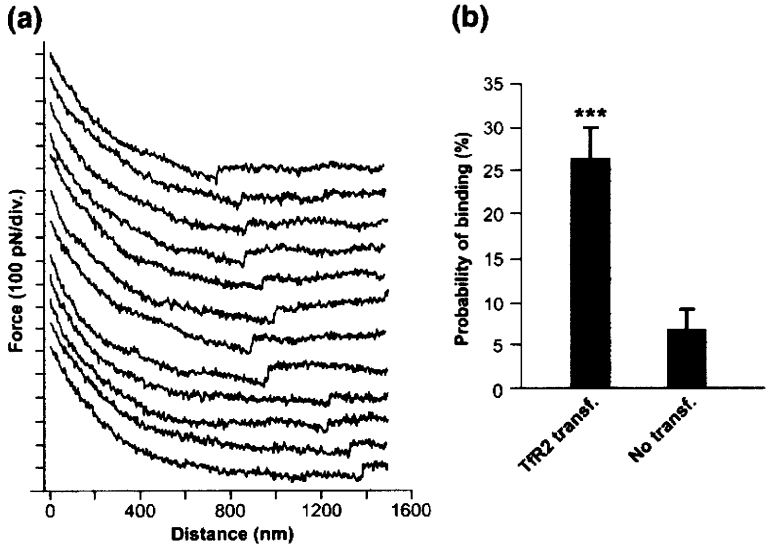

Fig. 4. (a) Retraction force curves on living HLF cells, transfected with TfR2α. The curves show specific unbinding events between Tf on the probe tip and TfR2α at the cell surface [in Tris-buffered saline (pH 7.4)]. (b) Specificity of detection by AFM. HLF cells (human hepatoma) were transiently cotransfected with TfR2α and GFP, and tested with a Tf-coated tip. The probability of binding was 26% ($n=7$ cells). In contrast, on nontransfected cells, the probability was only 6% ($n=12$ cells, $p<0.001$,***t test).

Force histogram for specific interaction between Tf and TfR2α

We recorded 1500 force curves with a Tf-coated tip on TfR2-transfected cells, allowing us to collect a total of 573 specific unbinding events in an experiment performed with a single tip using two cells. Events were analyzed and plotted in a force histogram (Fig. 5). A clear peak was visible on the histogram, showing that the mean unbinding force between Tf on the tip and TfR2 at the cell surface was 63±8 pN (at a mean loading rate of 2.8 nN/s). The experiment was repeated several days later using a new tip with cells independently cultured and gave similar results.

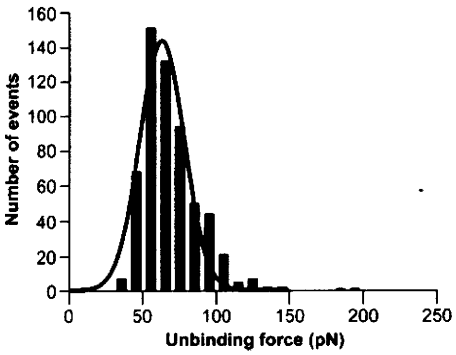

Fig. 5. Force histogram for the specific interaction between Tf and TfR2α on HLF cells. The histogram was obtained from an analysis of 573 unbinding events collected over 1500 force curves. The mean unbinding force is 63±8 pN for a mean loading rate of 2.8 nN/s. The gray line represents a Gaussian fit.

Dynamic force spectroscopy

Dynamic force spectroscopy, which consists of measuring the mean unbinding force at different loading rates, was performed with a Tf-coated tip on TfR2-transfected cells. As expected, the force was logarithmically dependent on the loading rate (Fig. 6). However, this dependence was small, as the force varied from 59±9 pN at a rate of 1.7 nN/s to 62±10 pN at a rate of 20 nN/s. In striking contrast, the unbinding force between TfR1 and Tf was reported at 39±5 pN at a rate of 1 nN/s and

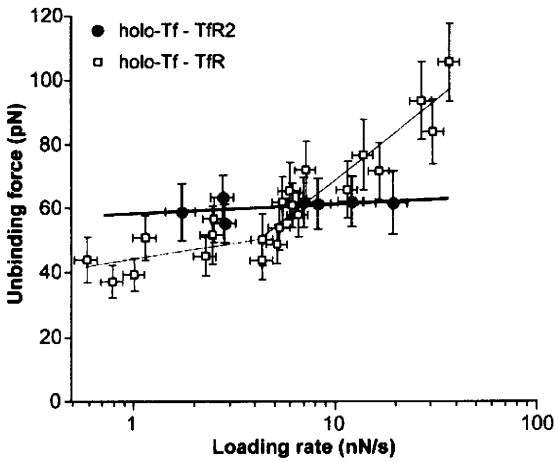

Fig. 6. Dynamic force spectroscopy of Tf TfR2α (black dots). The unbinding force is plotted as a function of the loading rate logarithm. For comparison, the force spectrum of Tf TfR1 is also shown. Only one regime is evident for TfR2, but two can be seen for TfR1, clearly revealing the different interactions of the two proteins with Tf.

increased up to 94±12 pN at a rate of 27 nN/s,[15] indicating that the binding of TfR2α and Tf differs from the binding of TfR1 and Tf. Furthermore, the force spectrum of TfR2-transfected cells displayed only one regime (slope), while two regimes were clearly visible for TfR1-expressing cells (Fig. 6), implying different interactions of Tf with TfR1 and TfR2.

Discussion

In their original publication, Kawabata *et al.* reported that TfR2α can bind Tf and donate iron to CHO cells,[13] therefore supporting cell growth.[14] Fleming *et al.* found that TfR2 expression is not regulated by intracellular iron status and thus might be involved in the pathogenesis of hemochromatosis.[18] Although TfR2 is thus shown to function in iron metabolism, its precise physiological role is still unknown.

To avoid confusion by TfR1, our first studies used HuH-7 cells with anti-sense suppressed TfR1 expression.[19,20] The amount of residual TfR1, however, was still high, so that it was not possible to differentiate between Tf binding to TfR1 and Tf binding to TfR2α because of the low affinity of TfR2α for Tf.[14] We therefore turned to TfR1-deficient CHO cells for expressing TfR2α.[13,21]

In the present study, the affinity of TfR2α for Tf was measured in living cells for the first time using [^{125}I]Tf to display the binding isotherm at 4 °C. The K_a for the binding of Tf by TfR2α was calculated to be 5.6×10^6 M^{-1}, about 35-fold less than that for the binding of Tf by TfR1 (2×10^8 M^{-1} to 3×10^8 M^{-1} in HuH-7 cells). The lower affinity of TfR2α in transfected CHO cells is in accordance with a previous report based on a qualitative study by flow cytometry.[14] Quantification by surface plasmon resonance using a recombinant soluble extracellular portion of the receptor gave a binding constant of 37×10^6 M^{-1}, consistent with the present result, considering the difference in methodology.[22] The deduced amino acid sequence of the extracellular domain of TfR2α protein is 45% identical and 66% similar to that of TfR1. TfR2α also possesses the RGD triad (amino acids 678 680),[13] which is thought to be critical for binding Tf to TfR1.[23] The lower affinity of TfR2α for Tf is now, therefore, not explicable.

Although the affinity of TfR2α for Tf is much less than that of TfR1, the concentration of iron-bearing Tf in the circulation (about 3×10^{-5} M) is sufficient to saturate TfR2α. TfR2α expression has been found in cells with active roles in iron metabolism. Liver, the principal organ of iron storage, expresses a high level of TfR2α mRNA, as do human hepatoma-derived HepG2 cells[13] and HuH-7 cells (unpublished observation). K562 cells, of human myelogenous erythroleukemic origin, also express TfR2α mRNA.[13] Studies of iron uptake from Tf prior to the discovery of TfR2 did not discriminate between the roles of the two receptors. In future studies, therefore, both receptors require consideration.

Binding of Tf to TRVb-TfR2α and TRVb mock cells at 4 °C was only 25 50% inhibited by a 100-fold excess of unlabeled Tf, possibly because of large, essentially nonsaturable binding. We therefore resorted to the use of a binding isotherm with terms for specific (saturable) and nonspecific (nonsaturable) binding to estimate the binding constants for each type of binding.[24] Curve-fitted parameters for specific binding attributable to transfected TfR2α were as follows: K_a, 5.6×10^6 M^{-1}; total number of sites, 2.8×10^4 $cell^{-1}$. These contrast with binding constants near 10^8 M^{-1} and site numbers in the range of 2×10^5 $cell^{-1}$ to 5×10^5 $cell^{-1}$ for Tf binding in K562 cells when TfR1 predominates and curve-fitting to a single class of sites adequately accounts for binding. An apparent binding constant of 6.5×10^9 M^{-1} is obtained for the nonsaturable binding of Tf to TRVb-TfR2α cells, substantially weaker than that derived for specific binding. At Tf concentrations of 10^{-6} M, for example, saturable binding would account for about 24,000 Tf molecules/cell, while nonsaturable binding would account for 6500 molecules/cell. Nevertheless, both TfR2α-dependent binding and nonspecific binding contribute to the association of Tf with the cells.

In the present study, CHO cells showed a receptor-independent association with Tf that should be considered when investigating the function of TfR2α expressed in CHO cells. We find a clear increase in cell-associated Tf after TfR2α expression. Since cell-associated Tf represents both cell-surface-bound Tf and Tf internalized via TfR2α, a proof of Tf internalization mediated by TfR2α was required. Cell-associated Tf persisting after acid washing confirmed the existence of Tf internalization via TfR2α.

After internalization, an efflux of Tf, without substantial degradation, is found. Thus, Tf internalized by TfR2α, like Tf internalized by TfR1, recycles. An important difference between the two receptors was observed in a pulse-chase study. Less than 12% of Tf bound to the cell surface of TRVb-TfR2α cells is internalized, with most of the Tf dissociated and released to the medium at 37 °C. In contrast, approximately 30 50% of membrane-bound Tf was internalized by human-hepatoblastoma-derived HepG2 cells[12] and human-hepatoma-derived HLF cells.[25] The lower affinity of TfR2α for Tf may help account for the difference between previous studies and the present work, since HepG2 and HLF cells express TfR1, but TRVb-TfR2α cells do not. In our pulse-chase study, no detectable internalization of membrane-bound Tf in a single cycle was found when the occupancy of TfR2α by transferrin was about 75%. In normal circulation, however, the concentration of iron-bearing Tf is close to 3×10^{-5} M, so that cell surface receptors are always saturated with Tf and replenished as Tf is internalized. TfR2α might therefore normally function in iron uptake from Tf, but this has yet to be experimentally confirmed.

Overexpressed TfR2α protein was also shown to mediate iron uptake, although its rate of iron donation was slow. We estimate, from the difference between iron uptake by TRVb-TfR2α cells and iron uptake by TRVb mock cells in Fig. 2b, that the rate of iron uptake was approximately 0.2 atom/receptor/min when cells were incubated with 8.1×10^{-7} M Tf. For comparison, the rate of iron uptake via TfR1 was about 0.5 1 atom/receptor/min in K562 cells. Thus, TfR2α may function in iron uptake from Tf, albeit with less efficiency than TfR1.

Because of the sequence similarities between TfR1 and TfR2α, the possibility that the protein monomers combine to form heterodimers was investigated. However, no detectable expression of heterodimers was found in the present studies. The possibility that our transfection procedure in HuH-7 cells yielded two different cell populations (one expressing TfR2α and the other failing to do so) must be considered, so that expression of heterodimers was too low for detection. We cannot exclude the possibility of heterodimer formation that might be detected by more sensitive methods or in other cells.

AFM was used to characterize the interactions between Tf and TfR2α protein at the single-molecule level. We found that the unbinding force needed to detach Tf from TfR2α (63±8 pN) was different from the unbinding force needed to detach Tf from TfR1, previously reported as 56± 7 pN.[15] However, dynamic force measurements revealed striking differences between Tf TfR1 and Tf TfR2α interactions, which reflected clearly distinct energy landscapes.[15] While Tf TfR1 unbinding is characterized by two energy barriers, only one is present for Tf TfR2. This obvious difference might arise from different binding points for Tf TfR1 and Tf TfR2α interactions. In addition, this possibility provides a structural interpretation for the energy barriers postulated here. We speculate that the two barriers of the Tf TfR1 interaction stem from the binding of both lobes of Tf (C-lobe and N-lobe), whereas the single barrier of Tf TfR2α interaction originates from the binding of a single lobe, but we recognize that this speculation requires further investigation.

In conclusion, the present study shows that TfR2α protein functions in binding Tf and taking up iron, and that there must be a difference between TfR1 and TfR2 in their interactions with Tf, as revealed by AFM. TfR2α mRNA lacks an iron responsive element, so that expression is not regulated by intracellular iron status[18] but possibly by cell cycle.[14] Furthermore, TfR2 cannot compensate for TfR1 in TfR1 knockout mice, which lack a functional Tf cycle and do not survive gestation.[26] A nonsense mutation of the human TfR2 gene causes a hemochromatosis-like disorder.[27,28] The physiological functions of TfR2 are therefore still unclear, although it likely contributes to the regulation of cellular iron status.

Materials and Methods

Cells and cell culture

TfR1-deficient CHO TRVb cells[21] were grown in F-12 Nutrients Mixture (Invitrogen, Grand Island, NY) supplemented with 5% heat-inactivated fetal bovine serum (Gemini Bio-Products, Woodland, CA), 100 U/ml penicillin, and 100 μg/ml streptomycin. All cultures were maintained at 37 °C in 5% CO_2.

TfR2α expression vector

Total RNA was extracted from K562 cells using the RNAgent Total RNA Isolation System (Promega, Madison, WI) following the manufacturer's instructions. Complementary DNA was reverse-transcribed from 1 μg of RNA using an oligo-dT primer (Promega) and MMLV reverse transcriptase (Stratagene, La Jolla, CA), and human TfR2α cDNA was amplified by hot-start PCR. A FLAG sequence was added to the 5′-terminus of the cDNA to enable detection of expressed protein by anti-FLAG antibodies. The oligonucleotides used as PCR primers were 5′-ACCTTAAGGCCACCATGGATTACAAGGATGACGACGATAAGATGGAGCGGCTTTG-3′ and 5′-GGTTCGAAGCAATGAGAGGTGGAC-3′. The conditions for amplification were as follows: 40 cycles of 99 °C for 1 min, 65 °C for 2 min, and 72 °C for 5 min. The amplified DNA fragment was digested with AflII and BstBI, and then inserted into the bicistronic mammalian expression vector pIRESpuro2 (Clontech, Palo Alto, CA). The orientation and sequence of the inserted TfR2α cDNA fragment were confirmed by sequencing.

Transfection

TRVb cells were grown in 35-mm six-well plates until they had reached 70 80% confluence, then they were transfected with the TfR2α expression vector using Lipofectamine Plus (Invitrogen, Carlsbad, CA). Selection was performed with 10 μg/ml puromycin (Clontech) for 2 weeks, and then the concentration of the antibiotic was raised to 30 μg/ml in order to isolate a clone with high-level expression of TfR2α. After another 2 weeks, one viable colony (TRVb-TfR2α) was obtained and then subcultured using a cloning cylinder. As mock-transfected controls, TRVb cells were transfected with the pIRESpuro2 vector without a cDNA insert, and one clone was isolated after 4 weeks of selection (TRVb mock cells). These transfectants were maintained at 30 μg/ml puromycin after isolation. Expression of TfR2α mRNA was confirmed by reverse transcriptase PCR, and the expression of TfR2α protein was confirmed by immunoprecipitation Western blot analysis using anti-FLAG antibodies (data not shown).

Total protein content

The total protein contents of TRVb, TRVb-TfR2α, and TRVb mock cells were determined with the Bio-Rad Protein Assay Kit (Bio-Rad, Hercules, CA) using bovine serum albumin (BSA) as standard. Cells were counted with a hemocytometer.

Iodination of Tf

Human Tf (Boehringer-Mannheim, Germany) was labeled with ^{125}I (Amersham Pharmacia Biotech, Piscataway, NJ) by the iodine monochloride method of McFarlane.[29] To remove unbound ^{125}I, we passed labeled Tf through a 10-DG desalting column (Bio-Rad) two times. Specific activities were observed in the range of 100 200 cpm/ng Tf, and more than 95% of ^{125}I was protein-bound as determined by precipitation with 20% TCA/4% PTA.

^{59}Fe labeling of Tf

Iron was removed from Tf, and labeling with ^{59}Fe was carried out by previously described methods.[30] Specific activities were in the range of 2000 3500 cpm/ng Fe. In some experiments, apotransferrin was labeled with ^{125}I, as described above, and then loaded with ^{59}Fe.

Binding assay

Tf binding assays were performed as previously reported.[31] Cell numbers were calculated from protein concentrations determined with the Bio-Rad Protein Assay Kit. Each experiment was performed in triplicate. The total number of specific binding sites per cell and the K_a for the binding of Tf to these sites were estimated from nonlinear least-squares curve fitting to a saturable binding isotherm:[32]

$$\text{occupied sites} = \frac{\text{total sites} \times K_a[\text{Tf}]}{1 + K_a[Tf]}$$

from which it is also possible to calculate the fraction of sites occupied by Tf at any concentration of free Tf.

Tf and iron uptake

Cells were plated at a density of 1×10^6 cells/well in 35-mm six-well plates 24 h before the experiments. Cells were preincubated with F-12 three times for 10 min at 37 °C, chilled on ice for 30 min, and then incubated at 37 °C with F-12 containing 2% BSA and labeled Tf at indicated concentrations and times. Cells were then washed with ice-cold PBS five times and solubilized by 0.1% Triton X-100 for counting.

Acid washing of cells

To remove cell-surface-receptor-bound Tf, we washed cells with ice-cold PBS five times and then incubated them with ice-cold acid wash buffer [0.025 M citric acid, 0.025 M sodium citrate, 200 μM deferoxamine mesylate, and 0.15 M sucrose (pH 4.0)] for 3 min, followed by two 2-min incubations with ice-cold F-12 medium to remove cell-surface-bound apotransferrin. Finally, the cells were washed once more with ice-cold PBS. This method removed approximately 90% of surface-bound Tf in TRVb-TfR2α cells.

Efflux of Tf from cells

Cells, plated at a density of 1×10^6 cells/well in 35-mm six-well plates 24 h before the experiments, were preincubated with F-12 three times for 10 min at 37 °C, chilled on ice for 30 min, and then incubated with F-12 containing 2% BSA and 3.5×10^{-7} M ^{125}I-labeled Tf for 60 min at 37 °C. After acid washing, fresh F-12 medium was added, and cells were again incubated at 37 °C. At indicated times, F-12 media were collected, and cells were washed with ice-cold PBS and solubilized by 0.1% Triton X-100. Media and cell lysates were then taken for γ-counting. After counting, media were incubated with 10% TCA/2% PTA for 30 min on ice, and then centrifuged at 14,000 rpm in an Eppendorf centrifuge for 20 min. Tf degradations were calculated from the radioactivities of supernatants and precipitates.

Pulse-chase study

TRVb-TfR2α cells were incubated with 5.1×10^{-7} M [^{125}I]Tf, as previously described, for 1 h at 4 °C. Cells were then washed with ice-cold PBS five times. Fresh F-12 medium was added, and cells were incubated at 37 °C. At indicated times, cells were chilled on ice, and media were immediately collected. Cells were again washed with ice-cold PBS, and media were collected. Cells were then acid washed to quantify surface-bound Tf and solubilized for the measurement of intracellular Tf.

Immunoprecipitation Western blot analysis

Human-hepatoma-derived HuH-7 cells were transiently transfected with the TfR2α expression vector, as described above. At 48 h after transfection, 5×10^6 cells were washed with PBS five times and collected with a cell scraper. Harvested cells were dissolved in 40 μl of the cell extraction buffer of the Mammalian Cell Extraction Kit (BioVision Incorporated, Mountain View, CA) following the manufacturer's instructions for Western blot analysis without immunoprecipitation, or in 1.5 ml of lysis buffer [10 mM Tris HCl, 150 mM NaCl, 1% Nonidet P-40, 1 mM ethylenediaminetetraacetic acid, and 1 mM PMSF containing 1:2000 Protease Inhibitor Cocktail (Boehringer-Mannheim; pH 7.4)] for immunoprecipitation Western blot analysis. Freezing and thawing were performed three times, following which samples were centrifuged at 2700*g*. Protein G Sepharose (Amersham Biosciences, Uppsala, Sweden) was added, and preparations were incubated at 4 °C for 8 h, then centrifuged at 1500*g* for 5 min. Supernatants were then collected for incubation with anti-FLAG M2 antibody (Sigma), which recognizes FLAG at any location in the target protein, or with anti-TfR1 antibody (Zymed Laboratory, South San Francisco, CA) for 8 h at 4 °C. Protein G Sepharose was added, and incubation continued for an additional 8 h at 4 °C. Samples were centrifuged at 1500*g* for 5 min, and pellets were washed with PBS five times. Concentrated dye buffer was added, and final concentrations were adjusted to 10 mM Tris HCl, 1 mM ethylenediaminetetraacetic acid, 2.5% SDS, 5% β-mercaptoethanol, and 0.01% bromophenol blue (pH 8.0). Samples were then immersed in boiling water for 5 min and centrifuged at 20,000*g* for 5 min to remove precipitated material. Electrophoresis using a 12% gradient polyacrylamide gel and transfer to a nitrocellulose membrane were carried out. The membrane was incubated with anti-TfR2 antibody (9F8 1C11) (Santa Cruz Biotechnology, Inc., Santa Cruz, CA) diluted 1:200 or with anti-TfR1 antibody diluted 1:1000, and then with horseradish-peroxidase-conjugated goat anti-mouse IgG antibody (R&D Systems, Minneapolis,

MN) diluted 1:2000. SuperSignal West Pico Chemiluminescent Substrate (Thermo Scientific, Rockford, IL) was used as development substrate.

Atomic force microscopy

The details of the methods for investigation using AFM were previously reported.[15] In brief, the probe of AFM is a sharp tip placed at the end of a soft cantilever. A piezoelectric scanner allows the precise positioning of the tip relative to the sample. A laser beam reflected on the cantilever backside and detected by photodiodes is used to measure cantilever deflection. This signal is either used as feedback to control the scanner (imaging mode) or measured and converted into force (force spectroscopy mode). Since the cantilever is mounted under the scanner, the optical path is free, and AFM can be coupled to an optical microscope. Tf was linked to the AFM tip by a three-step functionalizing protocol. First, SiN tips are aminosilanized by exposure to APTES vapors. Second, a heterobifunctional polyethylene glycol linker is anchored to amino-group-bearing tips through its NHS end. Third, Tf is attached to the polyethylene glycol linker free end via a maleimide cysteine bond.

Measuring the interaction force between Tf and TfR2α by AFM

HLF cells (human hepatoma) were cotransfected with TfR2α and GFP for identification, as previously described.[33] A Tf-coated tip was brought in contact with the cell surface, allowing the proteins to bind. The tip was then retracted, resulting first in protein stretching, then unbinding. Cantilever deflections during one cycle are recorded in a force curve. A binding unbinding event between Tf and TfR2α is represented by a sawtooth pattern on the curve. It allows calculation of the force necessary to unbind the two proteins, using the cantilever spring constant (Hooke's law). The mean unbinding force is obtained by fitting a Gaussian curve to the force histogram. The error on the mean unbinding force is calculated by adding the standard deviation of the sample and the error resulting from the spring constant calibration (10%). Moreover, the unbinding force is related to the pulling rate by:

$$F^* = \frac{k_B T}{x} \ln\left(\frac{x}{k_0 k_B T}\right) + \frac{k_B T}{x} \ln(r_f)$$

where F^* is the most probable unbinding force, k_0 is the dissociation rate constant, r_f is the loading rate applied, x is the width of the energy barrier along the direction of the applied force, k_B is the Boltzmann constant, and T is temperature.

Acknowledgements

We are grateful to Dr. Timothy E. McGraw for providing the CHO TRVb cells used in this study. This work was supported, in part, by grants 1 PO1 DK55495 and 5 RO1 DK015056 from the National Institutes of Health, US Public Health Service, USA.

Supplementary Data

Supplementary data associated with this article can be found, in the online version, at doi:10.1016/j.jmb.2010.01.026

References

1. Kühn, L. C., McClelland, A. & Ruddle, F. H. (1984). Gene transfer, expression, and molecular cloning of the human transferrin receptor gene. *Cell*, **37**, 95 103.
2. Feder, J. N., Gnirke, A., Thomas, W., Tsuchihashi, Z., Ruddy, D. A., Basava, A. *et al.* (1996). A novel MHC class I-like gene is mutated in patients with hereditary haemochromatosis. *Nat. Genet.* **13**, 399 408.
3. Feder, J. N., Penny, D. M., Irrinki, A., Lee, V. K., Lebrón, J. A., Watson, N. *et al.* (1998). The hemochromatosis gene product complexes with the transferrin receptor and lowers its affinity for ligand binding. *Proc. Natl Acad. Sci. USA*, **95**, 1472 1477.
4. Lebrón, J. A., Bennett, M. J., Vaughn, D. E., Chirino, A. J., Snow, P. M., Mintier, G. A. *et al.* (1998). Crystal structure of the hemochromatosis protein HFE and characterization of its interaction with transferrin receptor. *Cell*, **93**, 111 123.
5. Waheed, A., Parkkila, S., Zhou, X. Y., Tomatsu, S., Tsuchihashi, Z., Feder, J. N. *et al.* (1997). Hereditary hemochromatosis: effects of C282Y and H63D mutations on association with β2-microglobulin, intracellular processing, and cell surface expression of the HFE protein in COS-7 cells. *Proc. Natl Acad. Sci. USA*, **94**, 12384 12389.
6. Roy, C. N., Penny, D. M., Feder, J. N. & Enns, C. A. (1999). The hereditary hemochromatosis protein, HFE, specifically regulates transferrin-mediated iron uptake in HeLa cells. *J. Biol. Chem.* **274**, 9022 9028.
7. Gunshin, H., Mackenzie, B., Berger, U. V., Gunshin, Y., Romero, M. F., Boron, W. F. *et al.* (1997). Cloning and characterization of a mammalian proton-coupled metal-ion transporter. *Nature*, **388**, 482 488.
8. Fleming, M. D., Romano, M. A., Su, M. A., Garrick, L. M., Garrick, M. D. & Andrews, N. C. (1998). Nramp2 is mutated in the anemic Belgrade (b) rat: evidence of a role for Nramp2 in endosomal iron transport. *Proc. Natl Acad. Sci. USA*, **95**, 1148 1153.
9. Gruenheid, S., Canonne-Hergaux, F., Gauthier, S., Hackam, D. J., Grinstein, S. & Gros, P. (1999). The iron transport protein NRAMP2 is an integral membrane glycoprotein that colocalizes with transferrin in recycling endosomes. *J. Exp. Med.* **189**, 831 841.
10. Klausner, R. D., Van Renswoude, J., Ashwell, G., Kempf, C., Schechter, A. N., Dean, A. & Bridges, K. R. (1983). Receptor-mediated endocytosis of transferrin in K562 cells. *J. Biol. Chem.* **258**, 4715 4724.
11. Dautry-Varsat, A., Ciechanover, A. & Lodish, H. F. (1983). pH and the recycling of transferrin during receptor-mediated endocytosis. *Proc. Natl Acad. Sci. USA*, **80**, 2258 2262.
12. Ciechanover, A., Schwartz, A. L., Dautry-Varsat, A. & Lodish, H. F. (1983). Kinetics of internalization and recycling of transferrin and the transferrin receptor in a human hepatoma cell line. Effect of lysosomotropic agents. *J. Biol. Chem.* **258**, 9681 9689.
13. Kawabata, H., Yang, R., Hirama, T., Vuong, P. T., Kawano, S., Gombart, A. F. & Koeffler, H. P. (1999). Molecular cloning of transferrin receptor 2. A new member of the transferrin receptor-like family. *J. Biol. Chem.* **274**, 20826 20832.

14. Kawabata, H., Germain, R. S., Vuong, P. T., Nakamaki, T., Said, J. W. & Koeffler, H. P. (2000). Transferrin receptor 2-alpha supports cell growth both in iron-chelated cultured cells and *in vivo*. *J. Biol. Chem.* **275**, 16618 16625.
15. Yersin, A., Osada, T. & Ikai, A. (2008). Exploring transferrin receptor interactions at the single-molecule level. *Biophys. J.* **94**, 230 240.
16. Chan, R. Y., Ponka, P. & Schulman, H. M. (1992). Transferrin-receptor-independent but iron-dependent proliferation of variant Chinese hamster ovary cells. *Exp. Cell Res.* **202**, 326 336.
17. Lawrence, C. M., Ray, S., Babyonyshev, M., Galluser, R., Borhani, D. W. & Harrison, S. C. (1999). Crystal structure of the ectodomain of human transferrin receptor. *Science*, **286**, 779 782.
18. Fleming, R. E., Migas, M. C., Holden, C. C., Waheed, A., Britton, R. S., Tomatsu, S. *et al.* (2000). Transferrin receptor 2: continued expression in mouse liver in the face of iron overload and in hereditary hemochromatosis. *Proc. Natl Acad. Sci. USA*, **97**, 2214 2219.
19. Trinder, D., Zak, O. & Aisen, P. (1996). Transferrin receptor-independent uptake of diferric transferrin by human hepatoma cells with antisense inhibition of receptor expression. *Hepatology*, **23**, 1512 1520.
20. Sasaki, K., Zak, O. & Aisen, P. (1993). Antisense suppression of transferrin receptor gene expression in a human hepatoma cell (HuH-7) line. *Am. J. Hematol.* **42**, 74 80.
21. McGraw, T. E., Greenfield, L. & Maxfield, F. R. (1987). Functional expression of the human transferrin receptor cDNA in Chinese hamster ovary cells deficient in endogenous transferrin receptor. *J. Cell Biol.* **105**, 207 214.
22. West, A. P., Jr., Bennett, M. J., Sellers, V. M., Andrews, N. C., Enns, C. A. & Bjorkman, P. J. (2000). Comparison of the interactions of transferrin receptor and transferrin receptor 2 with transferrin and the hereditary hemochromatosis protein HFE. *J. Biol. Chem.* **275**, 38135 38138.
23. Dubljevic, V., Sali, A. & Goding, J. W. (1999). A conserved RGD (Arg-Gly-Asp) motif in the transferrin receptor is required for binding to transferrin. *Biochem. J.* **341**, 11 14.
24. Osterloh, K. & Aisen, P. (1989). Pathways in the binding and uptake of ferritin by hepatocytes. *Biochim. Biophys. Acta*, **1011**, 40 45.
25. Ikuta, K., Fujimoto, Y., Suzuki, Y., Tanaka, K., Saito, H., Ohhira, M. *et al.* (2000). Overexpression of hemochromatosis protein, HFE, alters transferrin recycling process in human hepatoma cells. *Biochim. Biophys. Acta*, **1496**, 221 231.
26. Levy, J. E., Jin, O., Fujiwara, Y., Kuo, F. & Andrews, N. C. (1999). Transferrin receptor is necessary for development of erythrocytes and the nervous system. *Nat. Genet.* **21**, 396 399.
27. Camaschella, C., Roetto, A., Cali, A., De Gobbi, M., Garozzo, G., Carella, M. *et al.* (2000). The gene TFR2 is mutated in a new type of haemochromatosis mapping to 7q22. *Nat. Genet.* **25**, 14 15.
28. Roetto, A., Totaro, A., Piperno, A., Piga, A., Longo, F., Garozzo, G. *et al.* (2001). New mutations inactivating transferrin receptor 2 in hemochromatosis type 3. *Blood*, **97**, 2555 2560.
29. McFarlane, A. S. (1963). *In vivo* behavior of I-fibrinogen. *J. Clin. Invest.* **42**, 346 361.
30. Young, S. P. & Aisen, P. (1980). The interaction of transferrin with isolated hepatocytes. *Biochim. Biophys. Acta*, **633**, 145 153.
31. Zak, O., Trinder, D. & Aisen, P. (1994). Primary receptor-recognition site of human transferrin is in the C-terminal lobe. *J. Biol. Chem.* **269**, 7110 7114.
32. Klotz, I. M. & Hunston, D. L. (1971). Properties of graphical representations of multiple classes of binding sites. *Biochemistry*, **10**, 3065 3069.
33. Yersin, A., Hirling, H., Kasas, S., Roduit, C., Kulangara, K., Dietler, G. *et al.* (2007). Elastic properties of the cell surface and trafficking of single AMPA receptors in living hippocampal neurons. *Biophys. J.* **92**, 4482 4489.

 DOI 10.1002/prca.200900112 *Proteomics Clin. Appl.* 2009, *3*, 1256–1264

RESEARCH ARTICLE

Heterogeneous expressions of hepcidin isoforms in hepatoma-derived cells detected using simultaneous LC-MS/MS

Takaaki Hosoki[1], Katsuya Ikuta[1], Yasushi Shimonaka[2], Yusuke Sasaki[2], Hideyuki Yasuno[2], Kazuya Sato[1], Takaaki Ohtake[1], Katsunori Sasaki[3], Yoshihiro Torimoto[4], Keiji Saito[2] and Yutaka Kohgo[1]

[1] Division of Gastroenterology and Hematology/Oncology, Department of Medicine, Asahikawa Medical College, Asahikawa, Japan
[2] Kamakura Research Labs, Chugai Pharmaceutical Co., Ltd., Kamakura, Japan
[3] Department of Gastrointestinal Immunology and Regenerative Medicine, Asahikawa Medical College, Asahikawa, Japan
[4] Oncology Center, Asahikawa Medical College Hospital, Asahikawa, Japan

Hepcidin, a key regulator of iron homeostasis, is known to have three isoforms: hepcidin-20, -22, and -25. Hepcidin-25 is thought to be the major isoform and the only one known to be involved in iron metabolism; the physiological roles of other isoforms are poorly understood. Because of its involvement in the pathophysiology of hereditary hemochromatosis and the anemia of chronic disease, the regulatory mechanisms of hepcidin expression have been extensively investigated, but most studies have been performed only at the transcriptional level. Difficulty in detecting hepcidin has impeded *in vitro* research. In the present study, we developed a novel method for simultaneous quantification of hepcidin-20, -22, and -25 in the media from hepatoma-derived cell lines. Using this method, we determined the expression patterns of hepcidin isoforms and the patterns of responses to various stimuli in human hepatoma-derived cultured cells. We found substantial differences among cell lines. In conclusion, a novel method for simultaneous quantification of hepcidin isoforms is presented. Heterogeneous expressions of hepcidin isoforms in human hepatoma-derived cells were revealed by this method. We believe our method will facilitate quantitative investigation of the role hepcidin plays in iron homeostasis.

Received: June 3, 2009
Revised: July 13, 2009
Accepted: July 17, 2009

Keywords:
Hepatocyte / Hepcidin antimicrobial peptide / Iron metabolism / LC-MS/MS

Correspondence: Dr. Katsuya Ikuta, Division of Gastroenterology and Hematology/Oncology, Department of Medicine, Asahikawa Medical College, 2-1-1-1 Midorigaoka-Higashi, Asahikawa, Hokkaido 078-8510, Japan
E-mail: ikuta@asahikawa-med.ac.jp
Fax: +81-166-68-2469

Abbreviations: **Ct**, threshold cycle; **DFO**, desferrioxamine; **EMEM**, Eagle's minimum essential medium; **FAC**, ferric ammonium citrate; **HAMP**, hepcidin antimicrobial peptide; **holo-Tf**, holo-transferrin; **IL-1β**, interleukin-1β; **IL-6**, interleukin-6; **LPS**, lipopolysaccharide; **QC**, quality control; **qRT-PCR**, quantitative RT-PCR; **SRM**, selected reaction monitoring

1 Introduction

Hepcidin is a small peptide mainly produced by the liver, and it is thought to be the key regulator in iron homeostasis [1, 2]. Hepcidin binds to ferroportin, the mammalian iron exporter expressed on the basolateral side of enterocytes and on the cell surface of macrophages, thereby causing the internalization and degradation of ferroportin [3]. Hepcidin thus inhibits iron uptake from the gastrointestinal tract and iron release from reticuloendothelial cells, so that iron balance of the body is negatively regulated by hepcidin [1, 2]. Increased

hepcidin expression therefore leads to iron deficiency while decreased hepcidin expression causes iron overload.

Hepcidin is involved in several diseases, such as hereditary hemochromatosis and the anemia of chronic disease. In hereditary hemochromatosis, various mutations occur in genes such as *HFE*, *hemojuvelin*, and *transferrin receptor 2*, leading to decreased hepcidin expression despite generalized iron overload [4–6]. In contrast, in anemia of chronic disease, inflammatory cytokines such as interleukin-6 (IL-6) [7, 8] and interleukin-1β (IL-1β) [9, 10] upregulate hepcidin expression and thus cause iron-deficiency anemia.

Recently, the regulation of hepcidin expression has been intensively studied to reveal pathophysiological mechanisms involved in diseases in which iron metabolism is altered. For instance, the cytokine IL-6 increases hepcidin synthesis utilizing signal transducers and activators of transcription-3 during inflammation such as caused by systemic infections [11]. The bone morphogenic proteins (BMPs) are members of the transforming growth factor β superfamily, and BMPs have been proposed to be involved in hemojuvelin-mediated regulation of hepcidin synthesis [12]. However, almost all research on the regulation of hepcidin expression has been restricted to studying changes in transcription of the *hepcidin antimicrobial peptide* (*HAMP*) gene utilizing RT-PCR under various conditions.

Hepcidin is produced mainly by hepatocytes expressing the *HAMP* gene located on chromosome 19. The transcript of this gene is believed to produce a prepropeptide of 84 amino acids, and then the peptide is digested by furin, the intercellular convertase, and finally the mature form of hepcidin appears in the peripheral blood [13]. However, there is little information about the ratios of serum prohepcidin to mature hepcidin, and the secreted fraction of hepcidin to hepcidin retained intracellularly. In addition, kidney cells have been shown to produce hepcidin independently of the liver [14]. Therefore, there is no proof that *HAMP* transcript levels of the liver reflect total body secretion of hepcidin-25. Consequently, it is desirable that hepcidin be determined from peptide levels in the serum, in addition to transcriptional levels of the liver and other organs.

Three isoforms of mature hepcidin are known. A 25-amino acid peptide (hepcidin-25) is thought to be the major isoform [15], but other forms of hepcidin such as hepcidin-20 and -22 have been detected in human urine [16]. Only hepcidin-25 has been shown to cause the internalization and degradation of ferroportin. However, the possibility arises that hepcidin-20 and -22 have different physiological roles in homeostasis and their expressions are regulated independently from hepcidin-25. It is therefore desirable that hepcidin-20, -22, and -25 be separately quantified.

The first method for measuring prohepcidin, using ELISA, was reported by Kulaksiz *et al.* [17]. That method has been applied for the analysis of hepcidin expression levels, but there is little information about how and whether hepatocytes secrete prohepcidin into the blood [17]. Several groups have developed antibodies to detect and measure hepcidin, but difficulties for differentiation of hepcidin-20, -22, and -25 [18] persist. MS-based modalities have been used in recent years for measuring hepcidin. For instance, SELDI-TOF-MS has been used for semi-quantification [19, 20], and LC-MS/MS has been employed for quantification of hepcidin [21, 22]. These methods are applicable to assaying clinical samples such as blood and urine. Most recently, Ganz *et al.* reported development of an ELISA system for quantification of human serum hepcidin that is expected to be a powerful tool for clinical samples [23].

Experiments *in vitro* would also be valuable for investigating the complex molecular mechanisms regulating hepcidin expression. Detection and quantification of hepcidin in cell culture media has been difficult, probably due to its low concentration.

We therefore aimed to develop a sensitive new method for measuring hepcidin that can simultaneously measure hepcidin-20, -22, and -25 secreted in culture media by hepatoma-derived cells. We now report such a method, improving the MS-based modality that we previously reported [22]. We also determined the characteristics of hepcidin expression of various hepatoma cell lines using the new method, which can be applied to analyzing differences among hepatoma cells of varying lineage.

2 Materials and methods

2.1 Hepcidin standards

Human hepcidin-25 was obtained from the Peptide Institute (Osaka, Japan). Hepcidin-20, -22, and [$^{13}C_{18}$, $^{15}N_3$]-hepcidin-25 were synthesized at the Peptide Institute.

2.2 Chemicals

BMP2 and holo-transferrin (holo-Tf) were purchased from R & D Systems; IL-6 was obtained from Wako Pure Chemical Industries, Osaka, Japan. FBS was purchased from Japan Bioserum; Eagle's minimum essential medium (EMEM), DMEM, RPMI-1640 medium, L-glutamine, and sodium bicarbonate were purchased from Sigma-Aldrich. Penicillin–streptomycin solution were bought from Invitrogen. IL-1β was purchased from Wako Pure Chemical Industries; desferrioxamine (DFO), ferric ammonium citrate (FAC), lipopolysaccharide (LPS), and cobalt chloride were obtained from Sigma-Aldrich. Decanoyl-RVKR-CMK (furin inhibitor I) was purchased from Calbiochem (Darmstadt, Germany). All other chemicals and solvents were of analytical reagent grade.

2.3 Cell cultures

Human hepatoma-derived cell lines used in this study were HepG2, HuH-1, HuH-2, HuH-4, HuH-6, HuH-7, WRL68, HB611, Hep3B, HLE, HLF, SK-HEP-1, and human primary

hepatocytes derived from normal liver (Applied Cell Biology Research Institute).

HuH-4, HB611, and HuH-6 cells were incubated with RPMI1640; HuH-7 cells were incubated with DMEM. Other cells were incubated with EMEM. Those medium were supplemented with 10% FBS, 100 U/mL penicillin, and 100 μg/mL streptomycin. All cells were cultured at 37°C in a humidied incubator with 5% CO_2. In some experiments, FBS-free UltraCulture medium (Lonza, MD, USA) supplemented with 2 mM L-glutamine was used. HepG2 cells could survive in this serum-free medium for more than 3 days.

Cells at the density of 1×10^6 cells/mL were grown in 6-well plates for 24 h to almost 80% conuency in 2 mL of culture medium. Medium in each well was replaced by 2 mL of culture medium containing various stimulants and then incubated for 48 h. All cell lines were maintained with 20 ng/mL IL-6 or 30 μM holo-Tf or no additives for control cells.

After 48 h, culture media were collected and analyzed for hepcidin-20, -22, and -25 concentrations as follows: 50 μL of 4% trichloroacetic acid solution containing 200 ng/mL [$^{13}C_{18}$, $^{15}N_3$]-hepcidin-25 as internal standard was added to an equal amount of each culture medium, mixed vigorously, and centrifuged. A 20-μL aliquot of the resulting supernatant was analyzed quantitatively by LC-MS/MS. Cells were lysed with 0.1% Triton X-100 for protein assay, or by Sepazol™ (Nacarai Tesque, Japan) for RT-PCR studies.

HepG2 cells were also treated with various reagents instead of IL-6 or holo-Tf, such as 200 pg/mL IL-1β, 100 μM DFO, 100 μM FAC, 1 μg/mL LPS, 50 μM $CoCl_2$, or 50 μM furin inhibitor I. After 48 h, culture media were collected for quantification of hepcidin isoforms, and cells were lysed for measuring protein concentrations.

Each treatment was performed in triplicate, and data presented as mean and SD.

2.4 LC/ESI-MS/MS analysis

LC/ESI-MS/MS was performed using an API4000QTRAP (Applied Biosystems, Foster City, CA, USA) equipped with a UPLC ACQUITY™ systems (Waters). The turboionspray was operated in the positive ion mode at 5500 V for the ion spray voltage. Analytical chromatography of human hepcidin-20, -22, and -25 was accomplished on a PLRP-S column (5 μm, 300 Å, 150 mm × 2.0 mm id; Polymer Laboratories, Shropshire, UK). Instrument control and data processing were with Analyst™ software version 1.4 (Applied Biosystems).

2.5 Quantitative analysis of human hepcidin-20, -22, and -25

Selected reaction monitoring (SRM) transitions were as follows: human hepcidin-20, m/z 548.85 → 119.80; human hepcidin-22, m/z 610.14 → 119.80; human hepcidin-25, m/z 558.80 → 120.07; [$^{13}C_{18}$, $^{15}N_3$]-human hepcidin-25, m/z 563.11 → 109.60. The declustering potential for human hepcidin-20, -22, -25, and [$^{13}C_{18}$, $^{15}N_3$]-human hepcidin-25 were 50, 50, 81, and 81 V, respectively. The turboionspray source was maintained at a temperature of 600°C. Collision energies for human hepcidin-20, -22, -25, and [$^{13}C_{18}$, $^{15}N_3$]-human hepcidin-25 were 52, 59, 73 and 75 V, respectively. The collisional activation dissociation gas was set at 4. Mobile phase A was 0.1% aqueous formic acid, and mobile phase B was 0.1% formic acid in ACN. Gradient conditions were as follows: B 20% (0 min, 0.3 mL/min) → 20% (2.01 min, 0.3 mL/min) → 25% (5.00 min, 0.3 mL/min) → 25% (10.00 min, 0.3 mL/min) → 90% (10.01 min, 0.3 mL/min) → 90% (12.00 min, 0.3 mL/min) → 20% (12.01 min, 0.3 mL/min) → 20% (14.00 min, 0.3 mL/min).

Analysis of hepcidin-25 in the BMP2-stimulated HepG2 culture medium was performed on the 6520 quadrupole-TOF/MS (Agilent Technologies).

2.6 RNA isolation and quantitative RT-PCR

Total RNA was isolated and quantitative RT-PCR (qRT-PCR) was performed in a reaction mix containing TaqMan Universal PCR Master Mix No AmpErase UNG (Applied Biosystems), specific human *HAMP* primers, and probe (pre-validated Taqman gene expression assay, Applied Biosystems), and 100 ng of cDNA. All reactions were multiplexed with the housekeeping gene 18S, provided as a pre-optimized control probe (Applied Biosystems) enabling data to be expressed as delta threshold cycle (ΔCt) values (where ΔCt = Ct of 18 s subtracted from Ct of gene of interest). Reactions were as follows: 50°C for 2 min, 95°C for 10 min; then 60 cycles of 95°C for 15 s and 60°C for 1 min. All measurements were performed in triplicate, and relative *HAMP* mRNA expression was expressed as fold expression over the average of *HAMP* mRNA expression corresponding to the HepG2 cells.

2.7 Cellular protein assay

Cell were lysed with 0.1% Triton-X and total protein concentrations were determined using the Bradford reagent (BioRad, Hercules, CA, USA), following the manufacturer's instructions.

3 Results

3.1 Establishment of quantitative measurement of hepcidin isoforms

To improve further the method for quantifying small peptides by LC-MS/MS, we developed a quantitative and simultaneous method for hepcidin-20, -22, and -25 in

biological fluids. Upon optimization of SRM conditions, the most intense precursor ions were selected in each mass spectrum to detect hepcidin isoforms. Product ions were selected to maximize sensitivity and selectivity. Using EMEM supplemented with 10% FBS as matrix, various concentrations of synthetic hepcidin isoforms were spiked, and analyzed by LC-MS/MS. Isoform peaks were not interfered with by a blank matrix, indicating the method has good selectivity.

Our method was validated by specificity, linearity, lower limit of quantification, intra-assay precision, and accuracy. Calibration curves were constructed over the range 2–1000 ng/mL in the above matrix. Five replicates of 2, 5, 50, 500, and 1000 ng/mL of each isoform quality control (QC) samples were prepared and analyzed by LC-MS/MS.

There was no interference peak at retention time of each isoform, confirming good specificity (Fig. 1A). Linearity of the calibration curves by weighted ($1/x^2$) linear regression was excellent (correlation coefficient: $r = 0.9974$ for hepcidin-20, $r = 0.9937$ for hepcidin-22, $r = 0.9950$ for hepcidin-25; Fig. 1B). Accuracies of the back-corrected concentrations were within 87.4–109% for hepcidin-20, 80.1–110% for hepcidin-22, and 80.5–109% for hepcidin-25. The lower limits of quantification for each hepcidin isoform was 2 ng/mL. Coefficients of variance in intra-assay QC samples were 1.2–8.6% for hepcidin-20, 3.1–5.7% for hepcidin-22, and 1.5–7.0% for hepcidin-25. Accuracies for QC samples were 99.7–122.1% for hepcidin-20, 102.6–132.5% for hepcidin-22, and 99.1–141.2% for hepcidin-25. These results indicate that the method is adequate for quantifying hepcidin isoforms in culture media.

3.2 Detection of hepcidin isoforms in HepG2 media

In the SRM chromatogram of HepG2 medium analyzed by LC-MS/MS, peaks corresponding to the retention time of synthetic hepcidin-22 and -25, but not hepcidin-20, were detected. Peaks corresponding to hepcidin-22 and -25 were also detected and up-regulated in 100 ng/mL BMP2 stimulated HepG2 medium (Fig. 2A). No peaks corresponding to hepcidin-20 were founded in the chromatogram of HepG2 media at any tested conditions.

We tried to identify the component of the corresponding peak for hepcidin-25 in HepG2 medium. For that purpose, BMP2 medium was prepared because it contained a relatively high concentration of putative hepcidin-25, (65.9 ng/mL). Synthetic hepcidin-25 and BMP2 medium were analyzed by quadrupole-TOF/MS. The major precursor ions of synthetic hepcidin-25 ranged from $m/z = 558.4$–559.0. At the same retention time, precursor ions from BMP2 medium showed a similar distribution (Fig. 2B). Mass spectra of product ions were also similar. Several major common product ions were observed (Fig. 2C). Overall, synthetic hepcidin-25 and HepG2-derived peak components are similar in retention time and mass spectra of the

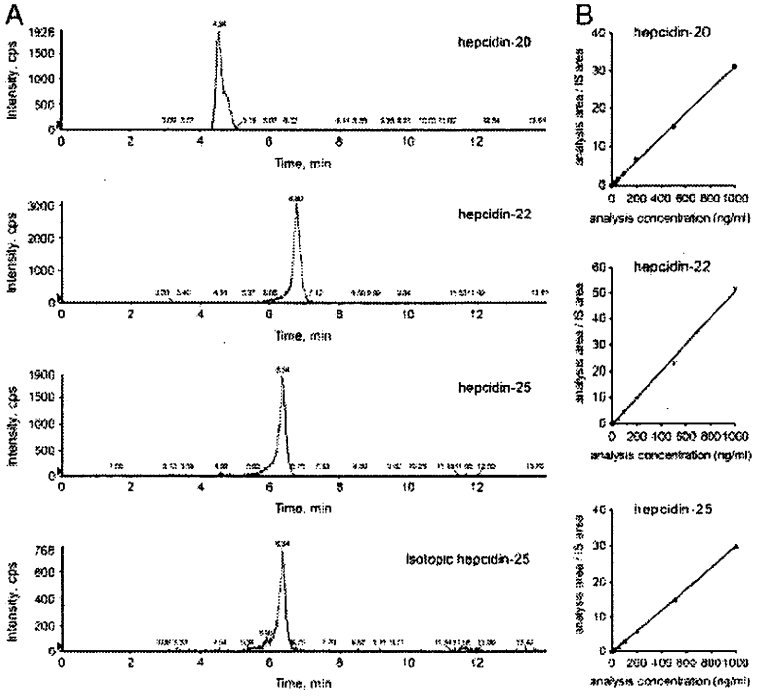

Figure 1. (A) Representative LC-MS/MS chromatograms of hepcidin-20, -22, -25, and blank isotopic hepcidin-25 sample. (B) The calibration curves of hepcidin-20, -22, and -25 in the culture medium are linear in the range of 2–1000 ng/mL. The correlation coefficients of calibration curves are as follows: hepcidin-20, $r = 0.9974$; hepcidin-22, $r = 0.9937$; hepcidin-25, $r = 0.9950$.

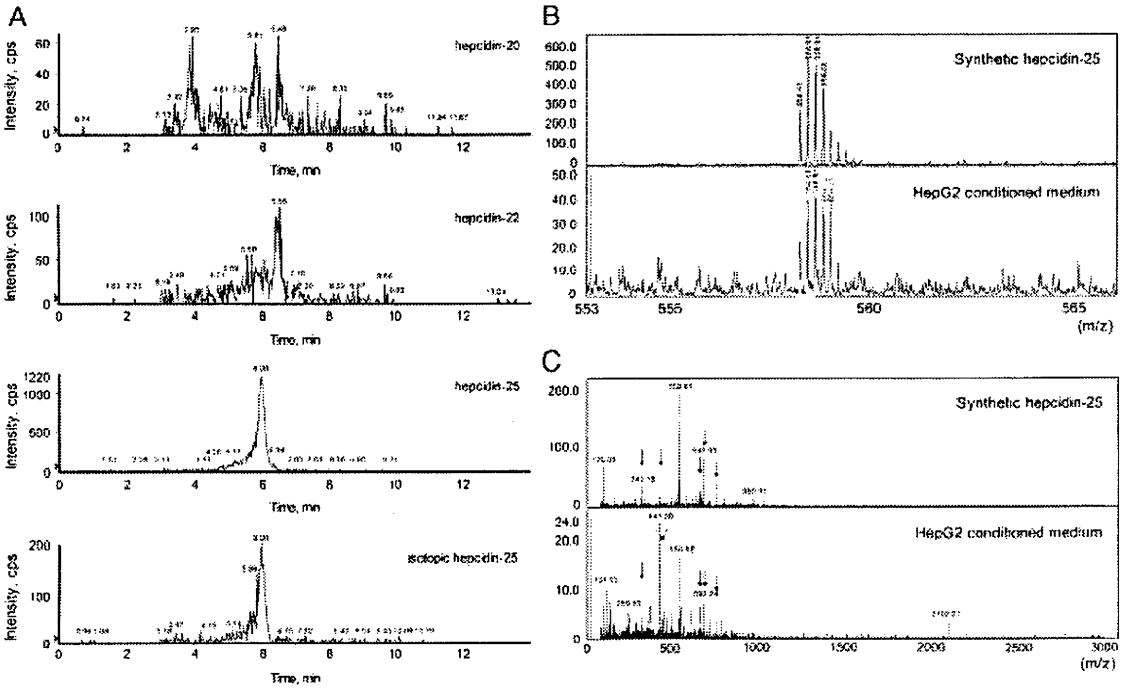

Figure 2. (A) Detection of hepcidin isoforms in BMP2-stimulated HepG2 medium. (B) MS spectra of synthetic hepcidin-25 and derived peak from BMP2-stimulated HepG2 medium showing similar patterns. (C) MS/MS spectra of synthetic hepcidin-25 and derived peak from BMP2-stimulated HepG2 medium showing similar patterns. Arrows show common fragments.

precursor ions and product ions, verifying that the peak detected in the culture medium represents hepcidin-25.

3.3 HAMP gene expressions in hepatoma-derived cell lines

We aimed at first to determine qualitatively whether cell lines derived from hepatocellular carcinomas express the *HAMP* gene as assayed by RT-PCR. Expression levels of *HAMP* mRNA differed among cell lines (Fig. 3A). HepG2, HuH-1, and HuH-7 cells showed relatively high *HAMP* mRNA expressions, but other cells exhibited only slight expressions. qRT-PCR was then performed (Fig. 3B). HepG2, HuH-1, and HuH-7 cells expressed high levels of *HAMP* mRNA, compatible with the results of qualitative RT-PCR. Only slight or moderate *HAMP* mRNA expression was found in other cells.

3.4 Quantification of hepcidin isoforms in the culture medium of various hepatoma-derived cell lines

HLE, HLF, SK-Hep1, and human primary hepatocytes did not show any detectable hepcidin isoforms in their culture media (data not shown). We could observe hepcidin isoforms in culture media from other cell lines. We also found that hepatoma-derived cell lines exhibited different patterns of hepcidin isoform expression and changes induced by various stimulations. Even among cell lines that secrete detectable hepcidin isoforms, four distinct patterns were discerned.

HepG2 cells expressed hepcidin-22 and -25, but not hepcidin-20. IL-6 significantly upregulated the expression of both isoforms, but holo-Tf suppressed hepcidin-25 expression (Fig. 4A).

WRL68 cells showed expression of hepcidin-20 and -22 even in control conditions, and holo-Tf stimulation increased both expressions significantly (Fig. 4B).

HuH-1 and HuH-7 cells expressed only hepcidin-25. IL-6 significantly increased the expression of hepcidin-25 in both cell lines. Addition of holo-Tf to the medium did not change the level of hepcidin-25 in HuH-1 cells, and even decreased hepcidin-25 in HuH-7 cells (Fig. 4C).

HB611, Hep3B, HuH-2, HuH-4, and HuH-6 showed expression of only hepcidin-20, but when holo-Tf was added, hepcidin-22 appeared (Fig. 4D).

We observed that some cell lines respond to holo-Tf by increasing the secretion of hepcidin-20 or -22. Although Lin *et al.* have reported *HAMP* mRNA expressions to be increased in mouse primary hepatocytes stimulated with

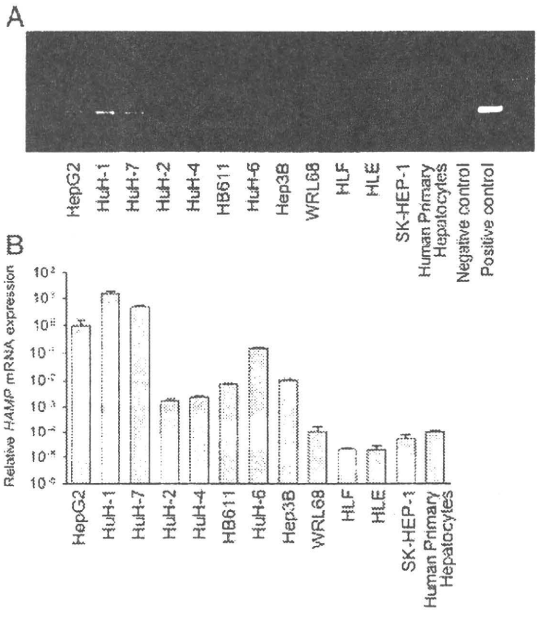

Figure 3. Expressions of *HAMP* mRNA in hepatoma-derived cell lines determined by qRT-PCR. (A) Qualitative RT-PCR showed that the expressions of *HAMP* mRNA were quite different among hepatoma-derived cell lines. (B) The expression levels of *HAMP* mRNA were standardized by 18*S* rRNA. Relative *HAMP* mRNA expression levels are shown as fold expression over the average of *HAMP* mRNA of HepG2 cells. HepG2, HuH-7, and HuH-1 cells highly express *HAMP* mRNA, while other cell lines exhibits only slight or moderate *HAMP* mRNA expressions.

human holo-Tf [24],] we believe ours is the first study showing upregulation of hepcidin at the peptide level by human holo-Tf in human cells. The physiological function of this effect is, however, not apparent since only hepcidin-25 is known to be involved in iron metabolism.

3.5 Determination of the changes of hepcidin expression in responses to various stimulations of HepG2 cells

The HepG2 cell line is one of the most frequently used hepatoma-derived lines for research and secretes mainly hepcidin-25, the only isoform reported to interact with ferroportin, into the culture medium.

Hepcidin expression has been reported to be regulated by inflammatory cytokines such as IL-6 and IL-1β; hence, HepG2 cells were stimulated with these cytokines. As shown in Fig. 5A, IL-6 significantly upregulates hepcidin-25, in agreement with earlier reports. A slight increase of hepcidin-22 was observed with IL-1β stimulation, but no obvious upregulation was seen in hepcidin-25. Iron overload has been reported to upregulate hepcidin expression *in vivo*, but addition of holo-Tf and FAC in the medium suppressed the expression of hepcidin-25. These results conflict with those of some *in vivo* investigations, but other transcriptional studies showed similar data to ours. Reasons for these discordances are still unknown.

Of interest, FAC increased hepcidin-22 expression by an unknown mechanism. DFO suppressed hepcidin-25 expression as expected change, but hepcidin-22 expression was increased. To investigate the effects of bacterial infections, LPS was added to media, and it significantly increased both hepcidin-22 and -25. Hypoxia is also reported to decrease hepcidin expressions [25], while in our studies $CoCl_2$ increased expression of both hepcidin-22 and -25. The furin inhibitor decreased hepcidin-25, but surprisingly hepcidin-22 was increased.

We then determined whether the inclusion of FBS influenced expressions of hepcidin types. Expressions of hepcidin-22 and -25 increased as higher concentrations of FBS were provided in the culture media, an effect that may have been due to the presence of cytokines in the FBS. HepG2 cells were then studied with various stimulants in FBS-free media. As shown in Fig. 5B, hepcidin expression levels were all lower than those determined in FBS-containing medium, and were almost at the limit of measurement by our method, but IL-6 upregulated hepcidin-25 expression. Holo-Tf and FAC depressed both hepcidin-22 and -25, as did the furin inhibitor. The finding that inclusion of FBS significantly influenced the expression of hepcidin deserves consideration from *in vitro* research using cultured cells.

4 Discussion

First developed for assaying prohepcidin [17], studies have used ELISA for measuring hepcidin in serum and urine. Lack of information about the physiological properties and importance of prohepcidin in clinical samples makes interpretation of these studies difficult. The main active isoform of hepcidin is believed to be hepcidin-25, but little information is available about how much translated prohepcidin in hepatocytes is released intact. In fact, Valore and Ganz have pointed out recently that most hepcidin released from the cells is the mature 25-residue form produced by furin [13]. Most recently, Ganz *et al.* developed a novel ELISA system for human serum hepcidin and it is expected that this method will be a powerful tool for clinical investigations, but it is unclear whether this method can be applied for *in vitro* research [23].

Methods utilizing MS-based modalities such as SELDI-TOF-MS have been widely used for measuring hepcidin in serum and urine samples [19]. However, the reliability of SELDI-TOF-MS for quantifying multiple molecules such as hepcidin isoforms is still unclear.

We recently developed a method utilizing LC/ESI-MS/MS for quantification of hepcidin [22]. We aimed to improve and extend this method to apply it for measurement of

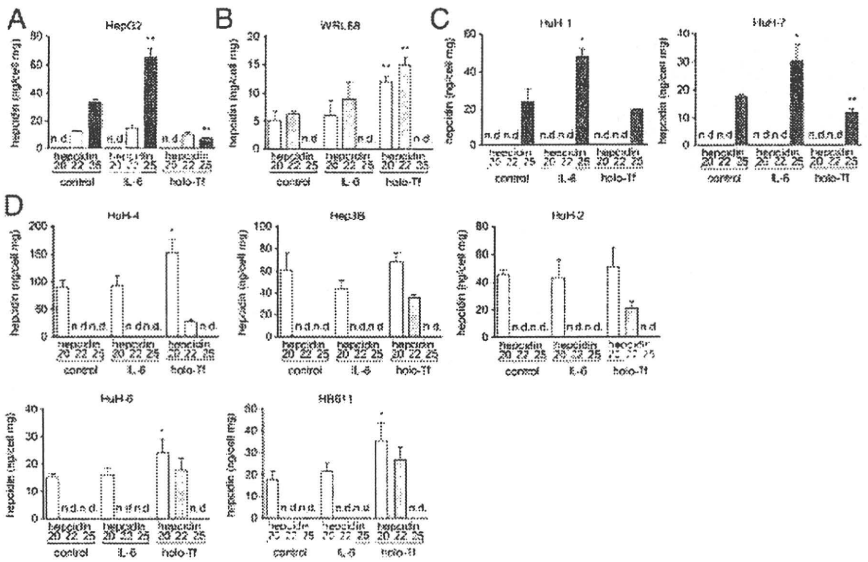

Figure 4. Quantification of hepcidin isoforms in the culture media of hepatoma-derived cell lines. The patterns of the expression of hepcidin isoforms were different among cell lines, and divided into four groups. (A) HepG2 cells, (B) WRL68 cells, (C) HuH-1 and HuH-7 cells, and (D) HB611, Hep3B, HuH-2, HuH-4, and HuH-6 cells. $^{*}p<0.05$, $^{**}p<0.01$, n.d.: not detected.

hepcidin secreted in culture media by hepatoma-derived cell lines. Our present assay, using MS with trichloroacetic acid precipitation, succeeds in this. Moreover, the new method can simultaneously detect and distinguish hepcidin-20, -22, and -25. The linear relationship between the peak area and hepcidin concentration provides simultaneous quantification of hepcidin-20, -22, and -25 isoforms. To our knowledge, this is the first report for simultaneous and quantitative measurement of hepcidin isoforms, applicable to evaluating hepcidin levels and their response to various stimulations for research using cultured cells. We believe that this method can be applied to clinical as well as research studies, thereby providing new information about hepcidin isoforms levels in serum. Determination of hepcidin isoforms may also be a biomarker for differential diagnosis and evaluation of disease activity in clinical studies, although further investigation is needed.

One advantage of our method is that it does not depend upon an antibody against hepcidin. Specificity of antibodies used for quantification of hepcidin requires validation to exclude the possibility that they recognize two or three isoforms of hepcidin simultaneously. Our method can also measure many samples in a relatively short time, so that it is useful for clinical samples and samples from *in vitro* research. However, it does require internal standards of hepcidin isoforms and mass spectrometers but still may be of interest in diverse laboratories.

We found differences in expression of *HAMP* mRNA among cell lines derived from hepatocytes. This finding indicates that such differences must be considered in using these cell lines for research in hepcidin expression.

HLE, HLF, and SK-HEP-1 cells exhibited low *HAMP* mRNA expression in qRT-PCR and did not secrete detectable hepcidin. They may have lost some physiological functions common to hepatocytes.

There were unexpected differences of secretion and response to various stimulations of hepcidin isoforms among cell lines. The cell lines that secreted detectable hepcidin in our study can be divided into at least four groups, suggesting that hepatocytes in the liver *in vivo* might possess different characteristics from each other. We believe this is the first report of the variety of hepcidin isoforms' expression patterns in hepatoma-derived cell lines. Possibly, one subset of hepatocytes is involved in only iron metabolism, while another line is involved in both iron metabolism and the antimicrobial system.

Care should be taken in evaluating hepcidin expression from transcriptional levels because we did not find any obvious correlation between *HAMP* mRNA expression and hepcidin secretion (Figs. 3 and 4). Moreover, different cell lines exhibit different patterns of hepcidin isoforms' secretion. Our data indicate that HuH-7 cells and Hep3B cells each express an mRNA of the *HAMP* gene as determined by RT-PCR. However, HuH-7 cells secrete only hepcidin-25 into the culture medium, and Hep3B cells secrete hepcidin-20 but no detectable hepcidin-25. These observations indicate a risk of misinterpretation if only transcriptional studies are performed for investigation of hepcidin expression, especially for *in vitro* research.

In this study, we subjected HepG2 cells to various stimulations, and observed changes of hepcidin-22 and -25 levels in culture media. The changes of hepcidin-22 and -25 were not parallel; therefore, again the determination of only *HAMP* mRNA might lead to misinterpretation, so simultaneous determination of hepcidin isoforms is strongly recommended. We observed changes of hepcidin-25 that are

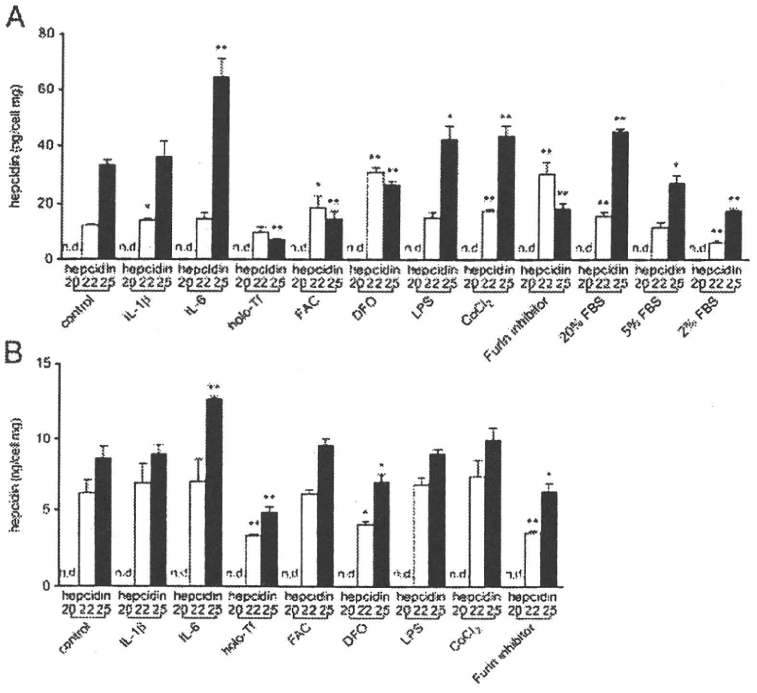

Figure 5. (A) Changes of hepcidin isoforms' expressions induced by various stimulations in the HepG2 cells. IL-6 (20 ng/mL), IL-1β pg/mL, holo-Tf (30 μM), FAC (100 μM), DFO (100 μM), $CoCl_2$ (50 μM), LPS (1 μg/mL), and furin inhibitor (50 μM) were added to the culture media of HepG2 cells as indicated. In addition, the effect of the concentrations of FBS on the expressions of hepcidin isoforms was determined. (B) HepG2 cells were incubated with serum-free medium UltraCulture. Hepcidin expression levels were all lower than those observed in FBS-containing medium. IL-6, IL-1β, holo-Tf, FAC, DFO, $CoCl_2$, LPS and furin inhibitor were also added to observe their effects on hepcidin isoforms' expressions. $^{*}p<0.05$, $^{**}p<0.01$, n.d.: not detected.

consistent with data previously reported elsewhere so that our method for quantification of hepcidin isoforms would be useful for investigating responses of hepatocytes to various stimulations. Observed changes that remain unexplained indicate a need for further investigation of the responses of hepatocytes to various stimulations in their expression of hepcidin isoforms.

We realize that varying concentrations of FBS might lead to different results even in the presence of identical stimulations. For example, the furin inhibitor decreased hepcidin-25 while hepcidin-22 was increased (Fig. 5A) in the presence of FBS. This suggests that the pathway for producing hepcidin-22 was activated when the pathway for producing hepcidin-25 was inhibited by furin inhibitor, thereby maintaining the total concentration of hepcidin although skewing the balance between isoforms. However, the precise mechanism of the effect is not known. Both hepcidin-22 and -25 were suppressed when cells were treated with furin inhibitor in FBS-free conditions (Fig. 5B), and this is contrary to the result observed in the presence of FBS. We speculated that the absence of FBS may stress the cells, increasing the sensitivity to furin inhibitor. We recognize that furin is a proprotein convertase acting on hepcidin expression at the posttranslational level [13], so that its inhibition should not be selectively affected by FBS. It is also possible, however, that unknown factors in FBS might upregulate hepcidin-22, since its concentration in FBS-free conditions could not be increased in our study. It may be advisable, therefore, to provide precisely controlled concentrations of FBS in further studies of expression of hepcidin isoforms *in vitro*, since FBS may already contain stimulants of hepcidin expression.

In conclusion, we have devised a method for simultaneous quantification of hepcidin-20, -22, and -25 in culture media by hepatoma-derived cell lines. Using this method, we determined the expression patterns of hepcidin isoforms and their responses to various stimulations in cultured cells, and we found that there are substantial differences among cell lines. We also found no obvious correlation between *HAMP* mRNA expressions and hepcidin isoforms' secretion. Levels of prohepcidin in the culture medium were too low to be detected by ELISA, indicating the necessity of directly measuring hepcidin instead of estimating it from prohepcidin measured by ELISA, especially *in vitro* studies. We believe that our method can contribute to *in vitro* research on the regulation of hepcidin expression, needed because the regulation of hepcidin expression is complex and difficult to investigate precisely *in vivo*.

The authors thank Dr. Philip Aisen for reviewing this manuscript.

The authors have declared no conflict of interest.

5 References

[1] Andrews, N. C., Forging a field: the golden age of iron biology. *Blood* 2008, *112*, 219–230.

[2] Ganz, T., Hepcidin, a key regulator of iron metabolism and mediator of anemia of inflammation. *Blood* 2003, *102*, 783–788.

[3] Nemeth, E., Tuttle, M. S., Powelson, J., Vaughn, M. B. *et al.*, Hepcidin regulates cellular iron efflux by binding to ferroportin and inducing its internalization. *Science* 2004, *306*, 2090–2093.

[4] Pietrangelo, A., Hemochromatosis: an endocrine liver disease. *Hepatology* 2007, *46*, 1291–1301.

[5] Papanikolaou, G., Samuels, M. E., Ludwig, E. H., MacDonald, M. L. *et al.*, Mutations in HFE2 cause iron overload in chromosome 1q-linked juvenile hemochromatosis. *Nat. Genet.* 2004, *36*, 77–82.

[6] Nemeth, E., Roetto, A., Garozzo, G., Ganz, T., Camaschella, C., Hepcidin is decreased in TFR2 hemochromatosis. *Blood* 2005, *105*, 1803–1806.

[7] Nemeth, E., Rivera, S., Gabayan, V., Keller, C. *et al.*, IL-6 mediates hypoferremia of inflammation by inducing the synthesis of the iron regulatory hormone hepcidin. *J. Clin. Invest.* 2004, *113*, 1271–1276.

[8] Nemeth, E., Valore, E. V., Territo, M., Schiller, G. *et al.*, Hepcidin, a putative mediator of anemia of inflammation, is a type II acute-phase protein. *Blood* 2003, *101*, 2461–2463.

[9] Lee, P., Peng, H., Gelbart, T., Wang, L., Beutler, E., Regulation of hepcidin transcription by interleukin-1 and interleukin-6. *Proc. Natl. Acad. Sci. USA* 2005, *102*, 1906–1910.

[10] Inamura, J., Ikuta, K., Jimbo, J., Shindo, M. *et al.*, Upregulation of hepcidin by interleukin-1beta in human hepatoma cell lines. *Hepatol. Res.* 2005, *33*, 198–205.

[11] Verga Falzacappa, M. V., Vujic Spasic, M., Kessler, R., Stolte, J. *et al.*, STAT3 mediates hepatic hepcidin expression and its inflammatory stimulation. *Blood* 2007, *109*, 353–358.

[12] Babitt, J. L., Huang, F. W., Wrighting, D. M., Xia, Y. *et al.*, Bone morphogenetic protein signaling by hemojuvelin regulates hepcidin expression. *Nat. Genet.* 2006, *38*, 531–539.

[13] Valore, E. V., Ganz, T., Posttranslational processing of hepcidin in human hepatocytes is mediated by the prohormone convertase furin. *Blood Cells Mol. Dis.* 2008, *40*, 132–138.

[14] Kulaksiz, H., Theilig, F., Bachmann, S., Gehrke, S. G. *et al.*, The iron-regulatory peptide hormone hepcidin: expression and cellular localization in the mammalian kidney. *J. Endocrinol.* 2005, *184*, 361–370.

[15] Nemeth, E., Preza, G. C., Jung, C. L., Kaplan, J. *et al.*, The N-terminus of hepcidin is essential for its interaction with ferroportin: structure–function study. *Blood* 2006, *107*, 328–333.

[16] Park, C. H., Valore, E. V., Waring, A. J., Ganz, T., Hepcidin, a urinary antimicrobial peptide synthesized in the liver. *J. Biol. Chem.* 2001, *276*, 7806–7810.

[17] Kulaksiz, H., Gehrke, S. G., Janetzko, A., Rost, D. *et al.*, Pro-hepcidin: expression and cell specific localisation in the liver and its regulation in hereditary haemochromatosis, chronic renal insufficiency, and renal anaemia. *Gut* 2004, *53*, 735–743.

[18] Merle, U., Fein, E., Gehrke, S. G., Stremmel, W., Kulaksiz, H., The iron regulatory peptide hepcidin is expressed in the heart and regulated by hypoxia and inflammation. *Endocrinology* 2007, *148*, 2663–2668.

[19] Tomosugi, N., Kawabata, H., Wakatabe, R., Higuchi, M. *et al.*, Detection of serum hepcidin in renal failure and inflammation by using ProteinChip System. *Blood* 2006, *108*, 1381–1387.

[20] Kartikasari, A. E., Roelofs, R., Schaeps, R. M., Kemna, E. H. *et al.*, Secretion of bioactive hepcidin-25 by liver cells correlates with its gene transcription and points towards synergism between iron and inflammation signaling pathways. *Biochim. Biophys. Acta* 2008, *1784*, 2029–2037.

[21] Murphy, A. T., Witcher, D. R., Luan, P., Wroblewski, V. J., Quantitation of hepcidin from human and mouse serum using liquid chromatography tandem mass spectrometry. *Blood* 2007, *110*, 1048–1054.

[22] Murao, N., Ishigai, M., Yasuno, H., Shimonaka, Y., Aso, Y., Simple and sensitive quantification of bioactive peptides in biological matrices using liquid chromatography/selected reaction monitoring mass spectrometry coupled with trichloroacetic acid clean-up. *Rapid Commun. Mass Spectrom.* 2007, *21*, 4033–4038.

[23] Ganz, T., Olbina, G., Girelli, D., Nemeth, E., Westerman, M., Immunoassay for human serum hepcidin. *Blood* 2008, *112*, 4292–4297.

[24] Lin, L., Valore, E. V., Nemeth, E., Goodnough, J. B. *et al.*, Iron transferrin regulates hepcidin synthesis in primary hepatocyte culture through hemojuvelin and BMP2/4. *Blood* 2007, *110*, 2182–2189.

[25] Nicolas, G., Chauvet, C., Viatte, L., Danan, J. L. *et al.*, The gène encoding the iron regulatory peptide hepcidin is regulated by anemia, hypoxia, and inflammation. *J. Clin. Invest.* 2002, *110*, 1037–1044.

doi:10.1111/j.1440-1746.2007.05290.x

METABOLISM, CANCER AND GENETICS

Dysregulation of systemic iron metabolism in alcoholic liver diseases

Yutaka Kohgo,* Takaaki Ohtake,* Katsuya Ikuta,* Yasuaki Suzuki,* Yoshihiro Torimoto* and Junji Kato†

*Division of Gastroenterology and Hematology/Oncology, Department of Medicine, Asahikawa Medical College, Asahikawa, and †Fourth Department of Internal Medicine, Sapporo Medical University, Sapporo, Japan

Yutaka Kohgo

Key words
alcohol, hepcidin, iron, steatohepatitis, transferrin receptor 1.

Correspondence
Professor Yutaka Kohgo, Division of Gastroenterology and Hematology/Oncology, Department of Medicine, Asahikawa Medical College, Asahikawa 078-8510, Japan. Email: yk1950@asahikawa-med.ac.jp

Abstract

Alcoholic liver diseases (ALD) are frequently associated with iron overload. Until recently, the effects of ethanol in hepatic iron uptake and intestinal iron absorption have not been clarified in detail. Two possible mechanisms for iron overload are the uptake of iron into hepatocytes in a specific manner through the increased expression of transferrin receptor (TfR) 1; and increased intestinal iron absorption by the lowering of hepcidin. It is worthwhile to examine whether a similar mechanism is present in the development of steatosis and non-alcoholic steatohepatitis (NASH). Hepatocytes have several iron uptake pathways. Ethanol increases transferrin (Tf)-mediated uptake via a receptor-dependent manner, but downregulates the non-Tf-bound iron uptake. According to immunohistochemical study, TfR1 was increased in hepatocytes in 80% of hepatic tissues of patients with ALD, but was not detected in normal hepatic tissues. In an experimental model, ethanol exposure to the primary cultured-hepatocytes in the presence of iron increased TfR1 expression and ^{59}Fe-labeled Tf uptake. In patients with ALD, intestinal iron absorption is increased by oral iron uptake assay. The regulatory hormone for iron homeostasis, hepcidin is downregulated in ethanol-loaded mice liver. As well as ALD, a similar mechanism was present in the mouse model fed with a high-fat diet, a model of the initial phenomenon of steatosis. The common mechanism for hepatic iron deposition and the triggering role of iron may be present in the development of ALD and non-alcoholic fatty liver disease/NASH.

Introduction

Body iron metabolism is strictly regulated in physiological conditions, but it is becoming clear that several factors including alcohol, hepatitis C virus (HCV) infection, steatohepatitis etc. affect iron metabolism and the outcomes of their own diseases.[1] Alcoholic liver diseases (ALD), which are characterized by fatty liver, fibrosis, hepatitis and cirrhosis, are frequently associated with mild to severe iron overload. In advanced cases, such as cirrhosis, the reticuloendothelial iron deposition is dominant, in which endotoxemia and hypercytokinemias are deeply involved. However, in ALD of earlier stages, such as fatty liver and fibrosis, iron deposition is very mild and iron is preferentially present in hepatocytes. These findings indicate that alcohol itself or its metabolites primarily affect and dysregulate overall body iron metabolism, including hepatocyte iron uptake and intestinal iron absorption in a specific manner such as via the newly discovered hormone, hepcidin. Concerning the fundamental pathogenesis of ALD, the production of reactive oxygen species (ROS) is considered to be responsible. During the oxidation process of ethanol, superoxide (O_2^-) is produced and is transformed to hydroxyl radical (OH^-), which is the most potent oxidant via the Fenton reaction in the presence of free iron.[2] Actually, in the intragastric infusion model of ALD, supplementation of carbonyl iron advances fibrosis and cirrhosis.[3] Two possible mechanisms of the role of alcohol in the early stage of disease can be seen in Fig. 1; one is increased uptake of iron into hepatocytes and the other is increased intestinal iron absorption.[4]

Iron accumulation in hepatocytes by ethanol

It is well known that Japanese patients with ALD have a phenotype that is rather mild compared with that of severe alcoholic siderosis seen in the USA.[5] In our study dealing with Japanese ALD,[6] as well as in the rat model,[7] there is a positive correlation between iron deposition and histological intensity of a lipid-peroxidation product, 4-hydroxy-2-nonenal (HNE)-protein adduct, suggesting that free iron responsible for the Fenton reaction may be present predominantly in hepatocytes, and that ROS-induced cell damage is increased.

Hepatocytes have several pathways for iron uptake: transferrin (Tf)-mediated and non-mediated pathways.[8] Plasma iron is usually bound to Tf and iron-bound Tf is taken up via its specific receptor. In addition, non-Tf-bound iron (NTBI) is thought to contribute iron uptake to hepatocytes through either a divalent metal transporter (DMT1)[9] or ZIP14.[10] As shown in Fig. 2, we have found that ethanol augmented ^{59}Fe-bound Tf, but inhibited ^{59}Fe-citrate

Journal of Gastroenterology and Hepatology **23** (2008) Suppl. 1; S78–S81

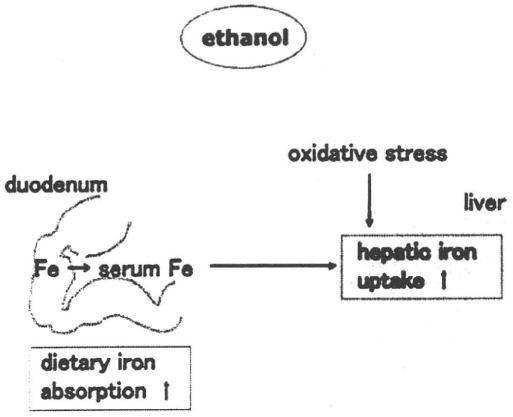

Figure 1 Two possible mechanisms of dysregulated hepatic iron accumulation in alcoholic liver disease (ALD) in the early stage of the disease. One is increased uptake of iron into hepatocytes and the other is increased intestinal iron absorption.

(NTBI), suggesting that Tf-bound iron may have an important role for hepatic iron uptake by ethanol. Although there are two molecules of Tf receptor, TfR1 and TfR2, TfR1 has a high affinity to serum Tf and is considered to be functional. However, in normal hepatocytes, TfR2 is constitutively expressed, but TfR1 is downregulated, suggesting that TfR1 does not contribute to the steady-state iron uptake. By immunohistochemical study of TfR1, the expression was increased in hepatocytes in 80% of hepatic tissues in Japanese patients with ALD, but was not detected in normal hepatic tissues.[11] It is noteworthy that the mean duration of abstinence of patients who demonstrated positive TfR1 expression in hepatocytes was significantly shorter than that of patients who demonstrated negative TfR1 expression. Taken together, it is possible that ethanol may augment TfR1. In the rat primary hepatocyte culture, the expression of TfR1 is upregulated in the presence of ethanol and iron by western blotting and ^{35}S-methionine metabolic labeling, suggesting that ethanol or its metabolite may affect the regulation of TfR1 and iron uptake. This increased TfR1 expression was regulated by increasing the activity of iron regulatory protein (IRP).[12]

Role of hepcidin in alcoholic iron overload

Body iron homeostasis is regulated strictly among processes such as dietary iron absorption, transport in circulation, and utilization or storage in bone marrow and liver. Increase in intestinal iron absorption is one of the mechanisms of the increase of body iron in alcoholics.[13] In patients with hereditary hemochromatosis, serum pro-hepcidin was lower than that in normal controls, suggesting that iron absorption is increased even with high iron storage.[14] It was also speculated that downregulation of hepcidin might be one of the important factors for the pathogenesis of iron overload in ALD.[15] In the ethanol-loaded mouse model which has a mild steatotic change, the hepcidin 1, 2 mRNA and protein expressions were significantly lower than in those of control.[16] In addition, alcohol-loading might disrupt the sensing signal of inflammatory cytokines and then downregulate hepcidin expression, following the increased iron absorption from the small intestine. Concerning the mechanism of hepcidin downregulation by alcohol, a decreased hepcidin expression in mouse liver is accompanied by increases of DMT1 and ferroportin 1, and a decrease of hepcidin promoter activity and DNA-binding activity of CCAAT/enhancer-binding protein (C/EBP).[17] In hemochromatotic hfe(-/-) mice treated with ethanol, a further decrease in hepcidin mRNA expression was observed, in association with the decrease of C/EBP alpha, which may have implications for the liver injury observed in alcoholic liver disease and genetic hemochromatosis in combination with alcohol.[18]

Steatosis as an inducer of dysregulation of iron metabolism

Non-alcoholic steatohepatitis (NASH) or non-alcoholic fatty liver disease (NAFLD) is a clinical entity characterized by the histopathological changes nearly identical to those induced by alcohol intake. In US population, approximately 25% are obese, and at least 20% of the obese individuals have hepatic steatosis, and it is suggested that obesity and steatosis affect liver disease progression.[19] A mild or moderate excess iron is frequently accumulated in liver tissue with NASH. Actually, the prevalence of the *HFE* gene mutation associated with hereditary hemochromatosis is increasing in patients with NASH, with the evidence strongly suggesting that iron is one of the important factors for the development of NASH.[20] It was also reported that phlebotomy is effective against NASH and the rise of oxidative stress markers related to the grade of iron overload in the liver.[21] However, the mechanism of iron overload in NASH is still unknown. Recently, our study using the high-fat diet mouse model suggested a strong link between the activation of peroxisome proliferator-activated receptor gamma (PPARγ) and the downregulation of cAMP response element-binding protein (CREB)[22] in addition to an increase of adipose differentiation-related protein (ADPR).[23] Among these molecules, the downregulation of CREB may be crucial, because CREB activation contributes to survival signals such as anti-apoptotic protein Bcl-2[24] and iron chelator desferrioxamine-increased CREB binding to the D-loop DNA of the mitochondrial genome in neurons.[25] The downregulation of CREB, which is associated with an activation of PPARγ by high-fat diet stimulation, may potentiate further dysregulation of iron metabolism. Actually, we found a significant increase in mRNAs of TfR1 and DMT1, and a decrease of hepcidin mRNA in association with bodyweight gain, mild steatosis and increased HNE immunostaining in this model (Miyoshi *et al.*, unpubl. data, 2007). As iron accumulation in the liver tissue after 16 weeks on a high-fat diet was not yet significant, our data strongly suggests that initial high-fat diet introduction upregulates TfR1 expression and downregulates hepcidin expression in the liver tissue, and upregulates DMT1 expression in the duodenum. Taken together, a high-fat diet itself has a capacity to accelerate intestinal iron absorption and hepatic iron uptake, as does ethanol. Therefore, it seems likely that iron is one of the important factors triggering NASH/NAFLD to develop, rather than a secondary factor.

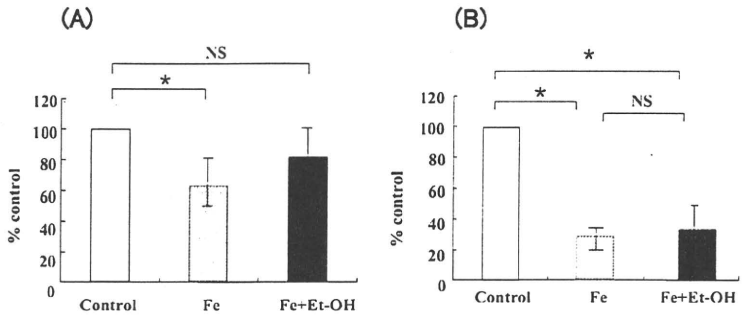

Figure 2 (a) Transferrin-bound iron uptake examined by incubation with ^{59}Fe-transferrin for 1 h after 24 h in the iron-deficient condition (control), with 20 μM iron (Fe), and with 20 μM iron and 25 mM ethanol (Fe + Et-OH). ^{59}Fe-transferrin uptake of iron-loaded hepatocytes was decreased to 63% compared with control hepatocytes. Additional ethanol exposure had a higher uptake at 82% of the control hepatocytes. There was no significant difference between control and iron- and ethanol-loaded hepatocytes. The experiment was repeated four times. (b) Non-transferrin-bound iron uptake examined by incubation with ^{59}Fe ferric chloride for 24 h in the iron-deficient condition (control), with 20 μM iron (Fe), and with 20 μM iron and 25 mM ethanol (Fe + Et-OH). Non-transferrin-bound ^{59}Fe uptake of iron-loaded hepatocytes was decreased to 29% compared with control hepatocytes. The additional ethanol exposure produced 34% of the iron uptake compared with the control hepatocytes. There was a significant difference between control and iron- and ethanol-loaded hepatocytes. The experiment was repeated four times. NS, not significant. *$P < 0.05$. (From [12] with modifications with authors' permission.)

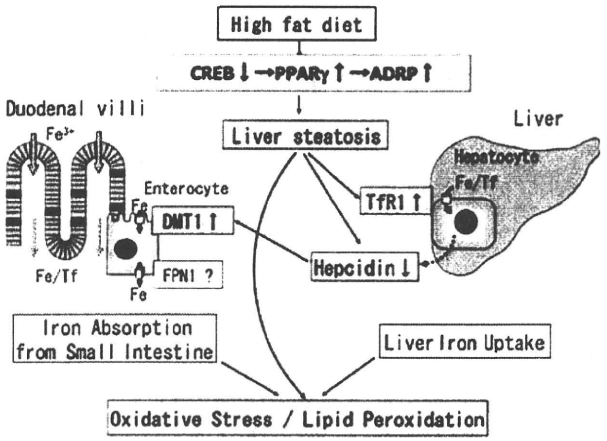

Figure 3 A high-fat diet itself has the capacity to accelerate intestinal iron absorption and hepatic iron uptake as well as ethanol. It seems likely that iron is one of the important factors triggering the development of non-alcoholic steatohepatitis/non-alcoholic fatty liver disease, rather than a secondary factor.

Conclusion

It is important to rationalize the finding of mild deposition of iron in earlier stages of ALD and to clarify the molecules involving the hepatic iron uptake in the presence of ethanol. In addition to the upregulation of TfR1 expression in hepatocytes, which is implicated in hepatic iron overload in alcoholic liver diseases, the decrease of hepcidin is also responsible for the increase of iron uptake. As shown in Fig. 3, a similar mechanism may be present in NASH or NAFLD through the production of ROS by a high-fat diet. A common pathway via steatosis/iron/oxidative stress should be considered for the development of liver fibrosis and carcinogenesis by iron as the initial progression stage.

Conflict of interest

No conflict of interest has been declared by the authors.

References

1 Kohgo Y, Ikuta K, Ohtake T, Torimoto Y, Kato J. Iron overload and cofactors with special reference to alcohol, hepatitis C virus infection and steatosis/insulin resistance. *World J. Gastroenterol.* 2007; **13**: 4699–706.
2 Bacon BR, Britton RS. The pathology of hepatic iron overload: a free radical- mediated process? *Hepatology* 1990; **11**: 127–37.
3 Tsukamoto H, Horne W, Kamimura S *et al.* Experimental liver cirrhosis induced by alcohol and iron. *J. Clin. Invest.* 1995; **96**: 620–30.
4 Kohgo Y, Ohtake T, Ikuta K *et al.* Iron accumulation in alcoholic liver diseases. *Alcohol. Clin. Exp. Res.* 2005; **29**: 189S–193S.
5 Takada A, Takase S, Tsutsumi M. Characteristic features of alcoholic liver disease in Japan: a review. *Gastroenterol. Jpn.* 1993; **28**: 137–48.
6 Ohhira M, Ohtake T, Matsumoto A *et al.* Immunohistochemical detection of 4-hydroxy-2-nonenal-modified-protein adducts in human alcoholic liver diseases. *Alcohol. Clin. Exp. Res.* 1998; **22**: 145S–149S.
7 Li CJ, Nanji AA, Siakotos AN, Lin RC. Acetaldehyde-modified and 4-hydroxynonenal-modified proteins in the livers of rats with alcoholic liver disease. *Hepatology* 1997; **26**: 650–7.
8 Breuer W, Hershko C, Cabantchik ZI. The importance of non-transferrin bound iron in disorders of iron metabolism. *Transfus. Sci.* 2000; **23**: 185–92.
9 Shindo M, Torimoto Y, Saito H *et al.* Functional role of DMT1 in transferrin-independent iron uptake by human hepatocyte and hepatocellular carcinoma cell, HLF. *Hepatol. Res.* 2006; **35**: 152–62.
10 Liuzzi JP, Aydemir F, Nam H, Knutson MD, Cousins RJ. Zip14 (Slc39a14) mediates non-transferrin-bound iron uptake into cells. *Proc. Natl Acad. Sci. USA* 2006; **103**: 13612–7.
11 Suzuki Y, Saito H, Suzuki M *et al.* Up-regulation of transferrin receptor expression in hepatocytes by habitual alcohol drinking is

implicated in hepatic iron overload in alcoholic liver disease. *Alcohol. Clin. Exp. Res.* 2002; **26**: 26S–31S.
12 Suzuki M, Fujimoto Y, Suzuki Y *et al.* Induction of transferrin receptor by ethanol in rat primary hepatocyte culture. *Alcohol. Clin. Exp. Res.* 2004; **28**: 98S–105S.
13 Duane P, Raja KB, Simpson RJ, Peters TJ. Intestinal iron absorption in chronic alcoholics. *Alcohol Alcohol.* 1992; **27**: 539–44.
14 Kulaksiz H, Gehrke SG, Janetzko A *et al.* Pro-hepcidin: expression and cell specific localisation in the liver and its regulation in hereditary haemochromatosis, chronic renal insufficiency, and renal anaemia. *Gut* 2004; **53**: 735–43.
15 Bridle K, Cheung TK, Murphy T *et al.* Hepcidin is down-regulated in alcoholic liver injury: implications for the pathogenesis of alcoholic liver disease. *Alcohol. Clin. Exp. Res.* 2006; **30**: 106–12.
16 Ohtake T, Saito H, Hosoki Y *et al.* Hepcidin is down-regulated in alcohol loading. *Alcohol. Clin. Exp. Res.* 2007; **31**: S2–8.
17 Harrison-Findik DD, Schafer D, Klein E *et al.* Alcohol metabolism-mediated oxidative stress down-regulates hepcidin transcripition and leads to increased duodenal iron transporter expression. *J. Biol. Chem.* 2006; **281**: 22 974–82.
18 Harrison-Findik DD, Klein E, Crist C, Evans J, Timchenko N, Gollan J. Iron-mediated regulation of liver hepcidin expression in rats and mice is abolished by alcohol. *Hepatology* 2007; **46**: 1979–85.
19 Harrison SA, Kadakia S, Lang KA, Schenker S. Nonalcoholic steatohepatitis: what we know in the new millennium. *Am. J. Gastroenterol.* 2002; **97**: 2714–24.
20 Bonkovsky HL, Jawaid Q, Tortorelli K *et al.* Non-alcoholic steatohepatitis and iron: increased prevalence of mutations of the HFE gene in non-alcoholic steatohepatitis. *J. Hepatol.* 1999; **31**: 421–9.
21 Nakashima T, Sumida Y, Furutani M *et al.* Elevation of serum thioredoxin levels in patients with nonalcoholic steatohepatitis. *Hepatol. Res.* 2005; **33**: 135–7.
22 Inoue M, Ohtake T, Motomura W *et al.* Increased expression of PPARgamma in high fat diet-induced liver steatosis in mice. *Biochem. Biophys. Res. Commun.* 2005; **336**: 215–22.
23 Motomura W, Inoue M, Ohtake T *et al.* Up-regulation of ADRP in fatty liver in human and liver steatosis in mice fed with high fat diet. *Biochem. Biophys. Res. Commun.* 2006; **340**: 1111–18.
24 Kitagawa K. CREB and cAMP response element-mediated gene expression in the ischemic brain. *FEBS J.* 2007; **274**: 3210–7.
25 Ryu H, Lee J, Impey S, Ratan RR, Ferrante RJ. Antioxidants modulate mitochondrial PKA and increase CREB binding to D-loop DNA of the mitochondrial genome in neurons. *Proc. Natl Acad. Sci. USA* 2005; **102**: 13 915–20.